Ultrasonographic measurements of fascicle length overestimate adaptations in serial sarcomere number

Avery Hinks[1], Martino Franchi[2,3], Geoffrey A. Power[1*]

[1]Department of Human Health and Nutritional Sciences, College of Biological Sciences, University of Guelph, 50 Stone Road East, Guelph, Ontario, Canada

[2]Department of Biomedical Sciences, Human Neuromuscular Physiology Laboratory, University of Padua, Padua, Italy

[3]CIR-MYO Myology Centre, University of Padua, Padua, Italy

Original Research Article

Running head: Muscle architecture of ultrasound-derived versus dissected fascicles

***Correspondence**
Geoffrey A. Power PhD.
Neuromechanical **P**erformance **R**esearch **L**aboratory
Department of Human Health and Nutritional Sciences
College of Biological Sciences
University of Guelph, Ontario, Canada
Telephone: 1-519-824-4120 x53752
Email: gapower@uoguelph.ca

Key Points Summary

- Measurements of muscle fascicle length via ultrasound are often used to infer changes in serial sarcomere number, such as increases following chronic stretch or resistance training, and decreases with aging or muscle disuse
- The present study used a rat model of casting the plantar flexor muscles in a stretched position to investigate directly whether ultrasound-derived fascicle length can accurately detect adaptations in serial sarcomere number
- Ultrasound detected an ~11% increase in soleus fascicle length, but measurements on dissected fascicles showed the actual increase in serial sarcomere number was only ~6%; therefore, measurements of ultrasound-derived fascicle length can overestimate serial sarcomere number adaptations by as much as 5%

Abstract

Ultrasound-derived measurements of muscle fascicle length (FL) are often used to infer increases (chronic stretch or training) or decreases (muscle disuse or aging) in serial sarcomere number (SSN). Whether FL adaptations measured via ultrasound can truly approximate SSN adaptations has not been investigated. We casted the right hindlimb of 15 male Sprague-Dawley rats in a dorsiflexed position (i.e., stretched the plantar flexors) for 2 weeks, with the left hindlimb serving as a control. Ultrasound images of the soleus, lateral gastrocnemius (LG), and medial gastrocnemius (MG) were obtained with the ankle at 90° and full dorsiflexion for both hindlimbs pre and post-cast. Following post-cast ultrasound measurements, legs were fixed in formalin with the ankle at 90º, then muscles were dissected, and fascicles were teased out for measurement of sarcomere lengths via laser diffraction and calculation of SSN. Ultrasound detected an 11% increase in soleus FL, a 12% decrease in LG FL, and an 8-11% increase in MG FL for proximal fascicles and at full dorsiflexion. These adaptations were partly reflected by SSN adaptations, with a 6% greater soleus SSN in the casted leg than the un-casted leg, but no SSN differences for the gastrocnemii. Weak relationships were observed between ultrasonographic measurements of FL and measurements of FL and SSN from dissected fascicles. Our results showed that ultrasound-derived FL measurements can overestimate an increase in SSN by ~5%. Future studies should be cautious when concluding a large magnitude of sarcomerogenesis from ultrasound-derived FL measurements, and may consider applying a correction factor.

Key Words: *Ultrasound, Sarcomere, Casting, Immobilization, Fascicle, Rats, Pennation angle*

Introduction

Characterization of a muscle's serial sarcomere number (SSN) gives insight into properties of biomechanical function (Lieber & Fridén, 2000; Narici *et al.*, 2016; Hinks *et al.*, 2022*a*). To that end, B-mode ultrasound is often used in humans to measure fascicle length (FL) and infer SSN adaptations at a smaller scale, such as increases in FL following resistance training (Blazevich *et al.*, 2007; Franchi *et al.*, 2014; Hinks *et al.*, 2021) or decreases in FL with age and disuse (Williams & Goldspink, 1978; Narici *et al.*, 2003; de Boer *et al.*, 2008; Power *et al.*, 2013). In animals, SSN can be estimated more precisely by dividing average sarcomere length (SL) measured via laser diffraction by the length of a dissected fascicle (Butterfield *et al.*, 2005; Chen *et al.*, 2020; Hinks *et al.*, 2022*b*). Unfortunately, direct measurement of SL in humans is invasive (Lieber *et al.*, 1997; Boakes *et al.*, 2007), and often prohibitively costly and not accessible (Lichtwark *et al.*, 2018; Adkins *et al.*, 2021). However, inferring SSN adaptations via ultrasound-derived measurements of FL may be problematic because apparent increases or decreases in FL could be due to longer or shorter SLs, respectively, at the joint angle in which FL was measured (Pincheira *et al.*, 2021). The relationship between SSN and FL may also depend on the region of muscle, with the human tibialis anterior displaying greater SSN in proximal fascicles due to a shorter SL (Lichtwark *et al.*, 2018). Collectively, the relationship between SSN and ultrasound-derived FL may depend on the joint angle and region of muscle at which measurements are taken. Whether FL adaptations measured via ultrasound truly approximate SSN adaptations has not been investigated.

Assessment of FL in rodents via ultrasound is less common than in humans, but not unfounded. Peixinho and colleagues developed reliable methods for assessment of muscle architecture via ultrasound in the rat plantar flexors (Peixinho *et al.*, 2011, 2014).

Ultrasonography of the rat plantar flexors also has enough sensitivity to detect morphological adaptations (Peixinho *et al.*, 2014; Mele *et al.*, 2016). These previous studies, however, only assessed pennation angle (PA) and muscle thickness, leaving characterization of ultrasound-derived FL adaptations in rats unclear. Altogether, rodent models present an opportunity to assess the sensitivity of ultrasound measurements of FL in detecting actual SSN adaptations.

The present study assessed the validity of ultrasound as a tool to detect adaptations in SSN. To do this, we immobilized the rat plantar flexors in a lengthened position—an intervention that rapidly increases soleus SSN (Tabary *et al.*, 1972; Williams & Goldspink, 1978; Soares *et al.*, 2007; Aoki *et al.*, 2009). We hypothesized that the ability for ultrasound-derived FL measurements to characterize adaptations in SSN would vary depending on the joint angle at which ultrasound measurements are obtained and the region of muscle.

Methods

Animals

Fifteen male Sprague-Dawley rats (sacrificial age ~19 weeks) were obtained (Charles River Laboratories, Senneville, QC, Canada). Approval was given by the University of Guelph's Animal Care Committee and all protocols followed CCAC guidelines (AUP #4905). Rats were housed at 23°C in groups of three and given ad-libitum access to a Teklad global 18% protein rodent diet (Envigo, Huntington, Cambs., UK) and room-temperature water. The right leg was immobilized in dorsiflexion for 2 weeks to place the plantar flexor muscles, in particular the soleus, in a lengthened position (Soares *et al.*, 2007; Aoki *et al.*, 2009). Per previous investigations of SSN adaptations in immobilized rat muscle, the contralateral limb served as a control (Heslinga & Huijing, 1993; Gomes *et al.*, 2004). Ultrasound images of the lateral gastrocnemius (LG), medial gastrocnemius (MG), and soleus were obtained at ~17 weeks of age (pre-immobilization) and ~19 weeks of age (post-immobilization).

Unilateral Immobilization

Using gauze padding, vet wrap, and a 3D-printed brace and splint, the right hindlimb of each rat was immobilized in dorsiflexion (40° ankle angle; full plantar flexion = 180°) (Figure 1A). Casts were inspected daily and repaired/replaced as needed. The toes were left exposed to monitor for swelling (Aoki *et al.*, 2009).

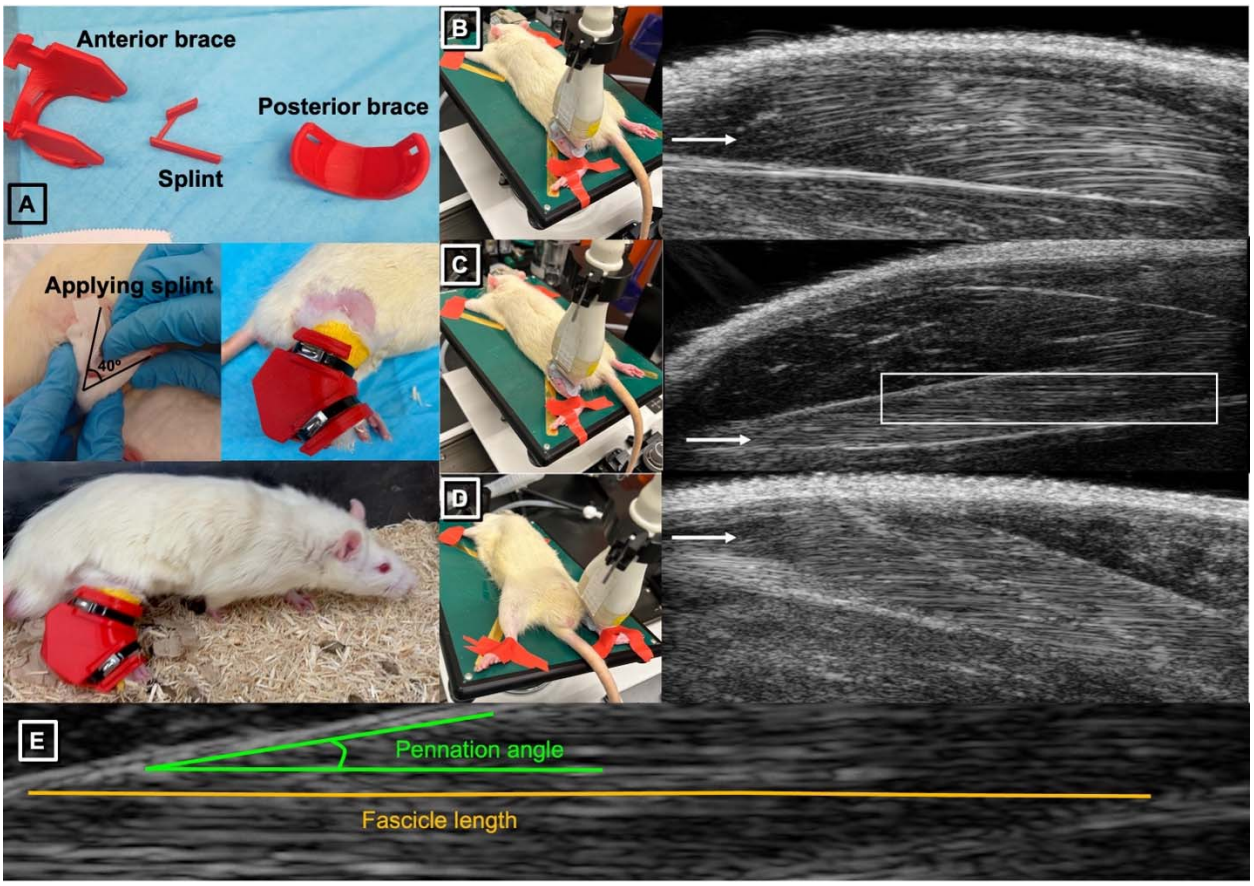

Figure 1: A. Example images of applying the splint and brace for the dorsiflexion cast. **B-D.** Setup and example of ultrasound images obtained from the left lateral gastrocnemius (B), soleus (C), and medial gastrocnemius (D), with the ankle fixed at 90° using tape. White arrows indicate the muscle of interest in each image. **E** corresponds to the area highlighted by the white box in C and shows representative tracings of fascicle length (orange) and pennation angle (green).

Ultrasonography

Ultrasound measurements were obtained from the right and left hindlimbs at pre-immobilization (no more than 1 week prior to first applying the casts) and post-immobilization (immediately following cast removal).

A UBM system (Vevo 2100; VisualSonics, Toronto, ON, Canada) operating at a centre frequency of 21 MHz was used to acquire images of the soleus, LG, and MG, with a lateral

resolution of 80 µm and an axial resolution of 40 µm (Mele *et al.*, 2016). A 23-mm long probe was used, allowing acquisition of images displaying muscle fascicles from end to end. During piloting, image acquisition was optimized with an image depth of 15 mm for the soleus and LG and 16 mm for the MG, both allowing a maximum frame rate of 16 Hz. Prior to image acquisition, rats were anesthetized using isoflurane. With the knee fully extended, tape was used to fix the ankles at two different positions for image acquisition: 1) 90º; and 2) full dorsiflexion. All ultrasound images were acquired by the same individual (A.H.). Images of the LG and soleus were obtained with the rat in a prone position and the hindlimb externally rotated, with the probe overlying the lateral aspect of the posterior shank (Figure 1B-C). Images of the MG were obtained with the rat in a supine position and the hindlimb externally rotated, with the probe overlying the medial aspect of the posterior shank (Figure 1D). The probe position was carefully adjusted to obtain the clearest possible view of fascicles in all of the proximal, middle, and distal regions of the muscle. Throughout image acquisition, the probe was stabilized by a crane with fine-tune adjustment knobs, minimizing pressure and limiting the error associated with human movement.

Ultrasound images were analysed using ImageJ software (Franchi *et al.*, 2020). ImageJ's multisegmented tool allowed careful tracing of the fascicle paths from end to end in measuring FL. Two measurements of FL and PA were obtained from each of the proximal, middle, and distal regions of each muscle (i.e., six FL and PA measurements per muscle). PA was defined as the angle between the fascicle and the aponeurosis at the fascicle's distal insertion point. All FL and PA measurements were obtained by the same experimenter (A.H.), who was blinded to the results until all measurements pre- and post-immobilization were obtained. During piloting, across three separate image acquisitions on the same rat, the coefficients of variation (standard

160 deviation / mean × 100%) for FL averaged among two measurements at each region of muscle
161 were all <10% (Table 1), which indicates low variation among repeated measures.

Table 1: Coefficients of variation for fascicle length across three separate image acquisitions on the same rat

Lateral gastrocnemius										
Day	**Proximal FL 1 (mm)**	**Proximal FL 2 (mm)**	**Proximal FL Average (mm)**	**Middle FL 1 (mm)**	**Middle FL 2 (mm)**	**Middle FL Average (mm)**	**Distal FL 1 (mm)**	**Distal FL 2 (mm)**	**Distal FL Average (mm)**	**Total FL Average (mm)**
1	11.79	11.79	**11.79**	12.96	13.10	**13.03**	12.69	12.00	**12.34**	**12.39**
2	10.25	12.75	**11.50**	12.78	13.59	**13.19**	12.26	13.68	**12.97**	**12.55**
3	12.56	11.30	**11.93**	12.61	13.03	**12.82**	14.56	12.85	**13.70**	**12.82**
CV (%)			**1.88**			**1.43**			**5.23**	**1.72**
Soleus										
Day	**Proximal FL 1 (mm)**	**Proximal FL 2 (mm)**	**Proximal FL Average (mm)**	**Middle FL 1 (mm)**	**Middle FL 2 (mm)**	**Middle FL Average (mm)**	**Distal FL 1 (mm)**	**Distal FL 2 (mm)**	**Distal FL Average (mm)**	**Total FL Average (mm)**
1	10.27	10.69	**10.48**	11.82	12.11	**11.97**	10.62	10.12	**10.37**	**10.94**
2	10.66	10.66	**10.66**	12.51	10.58	**11.55**	11.12	9.73	**10.42**	**10.88**
3	10.60	10.44	**10.52**	11.29	10.43	**10.86**	10.79	10.39	**10.59**	**10.66**
CV (%)			**0.91**			**4.88**			**1.10**	**1.37**
Medial gastrocnemius										
Day	**Proximal FL 1 (mm)**	**Proximal FL 2 (mm)**	**Proximal FL Average (mm)**	**Middle FL 1 (mm)**	**Middle FL 2 (mm)**	**Middle FL Average (mm)**	**Distal FL 1 (mm)**	**Distal FL 2 (mm)**	**Distal FL Average (mm)**	**Total FL Average (mm)**
1	10.52	11.93	**11.23**	12.42	13.47	**12.94**	13.06	12.50	**12.50**	**12.32**
2	11.11	12.36	**11.74**	12.33	13.56	**12.95**	13.45	12.91	**13.18**	**12.62**
3	10.66	10.88	**10.77**	11.86	13.60	**12.73**	13.76	12.31	**13.04**	**12.18**
CV (%)			**4.31**			**0.99**			**2.80**	**1.84**

FL = fascicle length

Serial Sarcomere Number Estimations

Following the post-immobilization ultrasound measurements, rats were sacrificed, and the hindlimbs were amputated and fixed in 10% phosphate-buffered formalin with the ankle pinned at 90° and the knee fully extended. After fixation for 1-2 weeks, the muscles were dissected and rinsed with phosphate-buffered saline. The muscles were then digested in 30% nitric acid for 6-8 hours to remove connective tissue and allow for individual muscle fascicles to be teased out (Butterfield *et al.*, 2005; Hinks *et al.*, 2022*b*).

For each muscle, two fascicles were obtained from each of the proximal, middle, and distal regions of the muscle (i.e., six fascicles total per muscle). Dissected fascicles were placed on glass microslides (VWR International, USA), then FLs were measured using ImageJ software (version 1.53f, National Institutes of Health, USA) from pictures captured by a level, tripod-mounted digital camera, with measurements calibrated to a ruler in plane with the fascicles (Supplemental Figure S1). Sarcomere length measurements were taken at six different locations proximal to distal along each fascicle via laser diffraction (Coherent, Santa Clara, CA, USA) with a 5-mW diode laser (25 μm beam diameter, 635 nm wavelength) and custom LabVIEW program (Version 2011, National Instruments, Austin, TX, USA) (Lieber *et al.*, 1984), for a total of 36 sarcomere length measurements per muscle. Serial sarcomere numbers was calculated as:

Serial sarcomere number = fascicle length / average sarcomere length

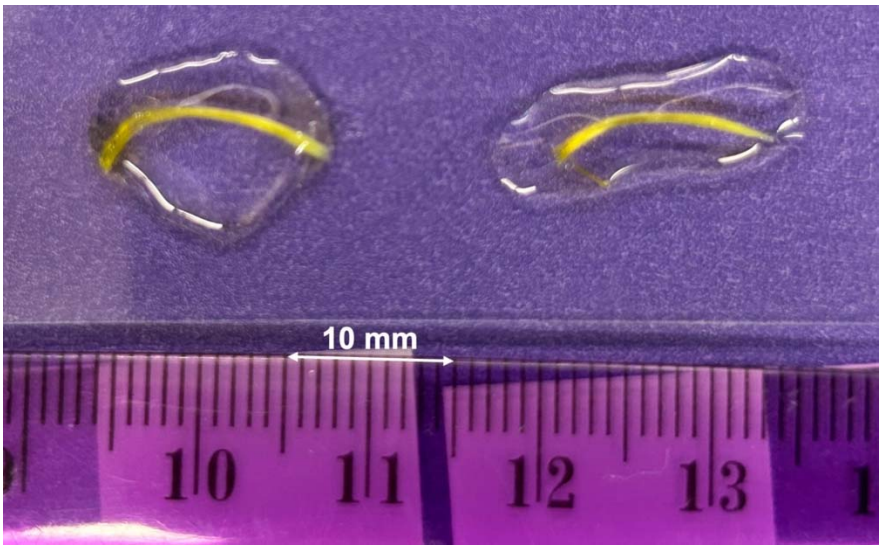

Supplemental Figure S1: Example of distal fascicles from the right lateral gastrocnemius used for measurement of dissected fascicle length and calculation of serial sarcomere number, with fascicles positioned in the same plane as a ruler used to set the scale.

Statistical Analysis

Statistical analyses were conducted using GraphPad Prism 9.5.1. To investigate variation in ultrasound-derived FL and PA, three-way analysis of variance (ANOVA) (time [pre-immobilization, post-immobilization] × joint position [90 degrees, full dorsiflexion] × region [proximal, middle, distal]) was performed for each muscle from each leg, with Geisser-Greenhouse corrections for sphericity. For each dissected muscle, a two-way ANOVA (leg [casted, un-casted] × region [proximal, middle distal] was used to investigate variation in SSN, SL, and FL, with Geisser-Greenhouse corrections for sphericity. For all ANOVAs, where interactions or effects of region were detected, pairwise comparisons (two-tailed paired t-tests) were performed with a Bonferonni correction for multiplicity. Two-tailed, paired t-tests compared muscle wet weights between the casted and un-casted leg, with a Bonferroni correction for multiplicity. For all significant t-tests, the effect size was reported as Cohen's d. Significance was set at $\alpha = 0.05$.

Linear regression was used to investigate the relationship between: 1) ultrasound-derived FL at 90° post-cast and FL of dissected fascicles; 2) ultrasound-derived FL at each joint angle post-cast and SSN of dissected fascicles; and 3) adaptations in ultrasound-derived FL (as % change pre to post-cast) at each joint angle and adaptations in SSN of dissected fascicles (as % change from the un-casted to the casted leg).

Results

Effects of region, joint position, and time on fascicle length measured via ultrasound

Three-way ANOVA results for FL measured via ultrasound are presented in Table 2.

For all muscles, there were effects of joint position, with FL increasing from a 90° ankle angle to full dorsiflexion (Table 2; Figures 2-4). For the gastrocnemii, there were effects of region, with FL increasing from proximal to distal (Table 2; Figures 2 and 4).

For ultrasound-derived FL of the un-casted LG, there was a joint position × time interaction (Table 2). Pairwise comparisons showed that FL decreased by 6% pre to post-cast when measurements were performed at 90° ($P = 0.0001$, $d = 0.45$), but did not change according to measurements performed at full dorsiflexion ($P = 1.00$) (Figure 2B).

For ultrasound-derived FL of the casted LG, there was an effect of time (Table 2), with FL decreasing by 12% pre to post-cast (Figure 2C).

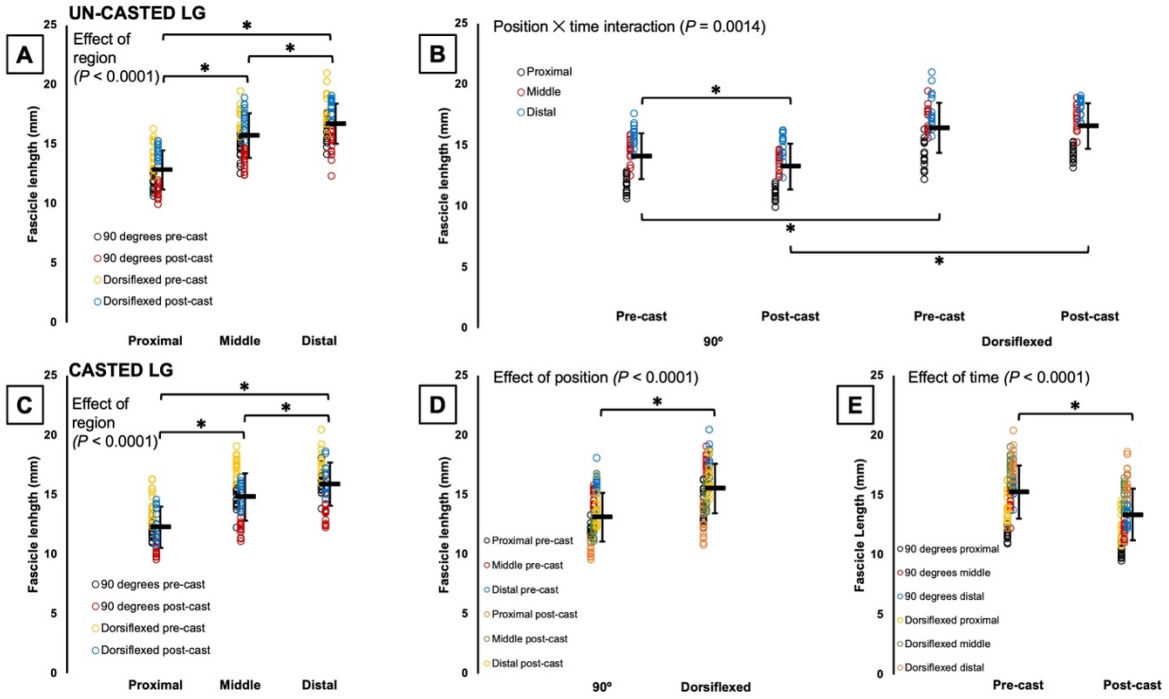

Figure 2: Fascicle length of the un-casted and casted lateral gastrocnemius (LG) measured via ultrasound. For the un-casted LG, there was an effect of region (A) and an interaction between joint position and time (B). For the casted LG, there were effects of region (C), joint position (D), and time (E). *Significant difference between indicated means ($P < 0.05$). Data are presented as mean ± standard deviation.

For ultrasound-derived FL of the un-casted soleus, there was a region × joint position interaction (Table 2). Pairwise comparisons showed distal fascicles were longer than proximal fascicles when measured at 90° ($P = 0.0413$, $d = 0.44$), but proximal and middle FL did not differ ($P = 0.194$), and middle and distal FL did not differ ($P = 1.00$) (Figure 3A). Conversely, in measurements performed at full dorsiflexion, middle fascicles were longer than proximal fascicles ($P = 0.0003$, $d = 0.65$), but proximal and distal FL did not differ ($P = 1.00$), and middle and distal FL did not differ ($P = 0.0591$) (Figure 3A). FL of the un-casted soleus did not change from pre to post-cast, with no effect of time (Figure 3B).

For the casted soleus, an effect of time showed that ultrasound-derived FL increased on average by 11% pre to post-cast (Table 2). There was also a region × time interaction. Pairwise

236 comparisons showed all regions of the soleus increased FL from pre to post-cast (proximal: P =
237 0.0301, d = 0.57; middle: $P < 0.0001$, d = 1.12; distal: $P < 0.0001$, d = 1.13) (Figure 3D). Pre-
238 cast, there were no regional differences in FL (P = 0.0849-1.00), but post-cast, middle ($P <$
239 0.0001; d = 1.01) and distal fascicles ($P < 0.0001$; d = 0.91) were longer than proximal fascicles
240 (Figure 3D). Accordingly, the increase in proximal FL from pre to post-cast was smaller (+6%)
241 than the increases in middle and distal FL (both +13%).
242

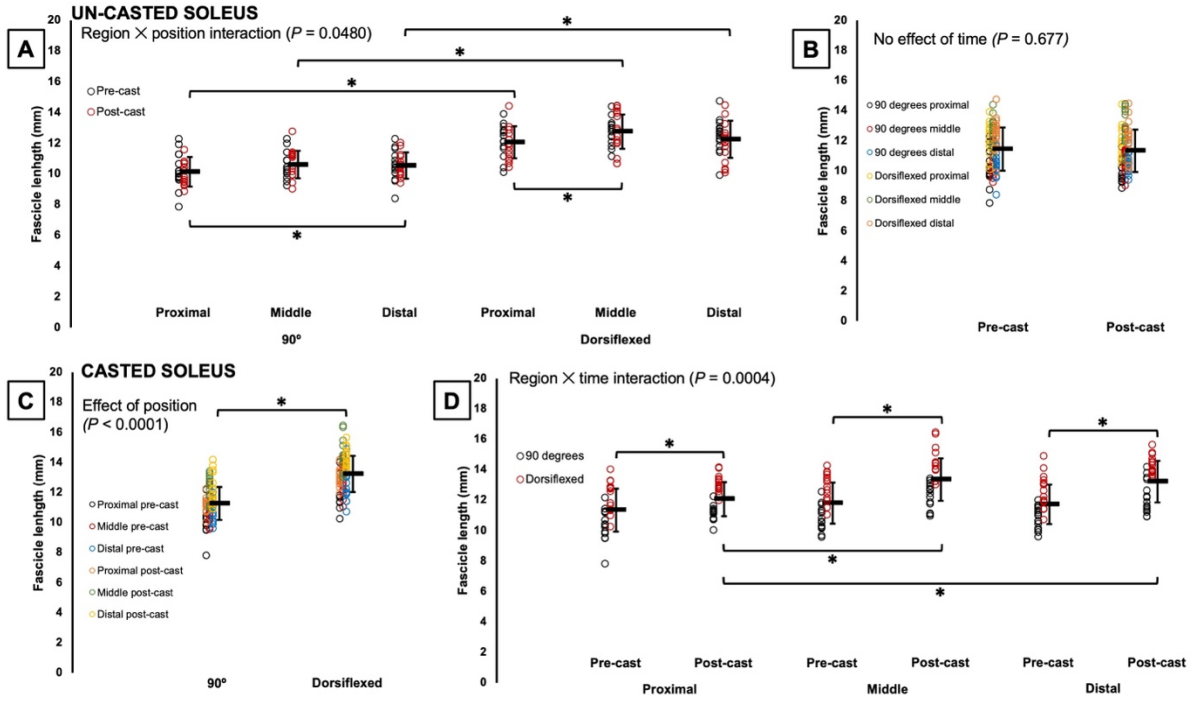

243

244 **Figure 3:** Fascicle length of the un-casted and casted soleus measured via ultrasound. For the un-
245 casted soleus, there was an interaction between region and position (A) and no effect of time (B).
246 For the casted soleus, there was an effect of position (C) and an interaction between region and
247 time (D). *Significant difference between indicated means ($P < 0.05$). Data are presented as
248 mean ± standard deviation.
249

250 For ultrasound-derived FL of the un-casted MG, there was a region × time interaction
251 (Table 2), with distal FL increasing by 8% pre to post-cast (P = 0.0330, d = 0.63) (Figure 4A).

For ultrasound-derived FL of the casted MG, there was also a region × time interaction (Table 2), but with proximal FL increasing by 11% pre to post-cast (P = 0.0028, d = 0.82) (Figure 4C). A joint position × time interaction showed that measurements at 90° detected no change in FL pre to post-cast (P = 1.00), but measurements at full dorsiflexion detected an 8% increase in FL (P = 0.0002, d = 0.76) (Figure 4D).

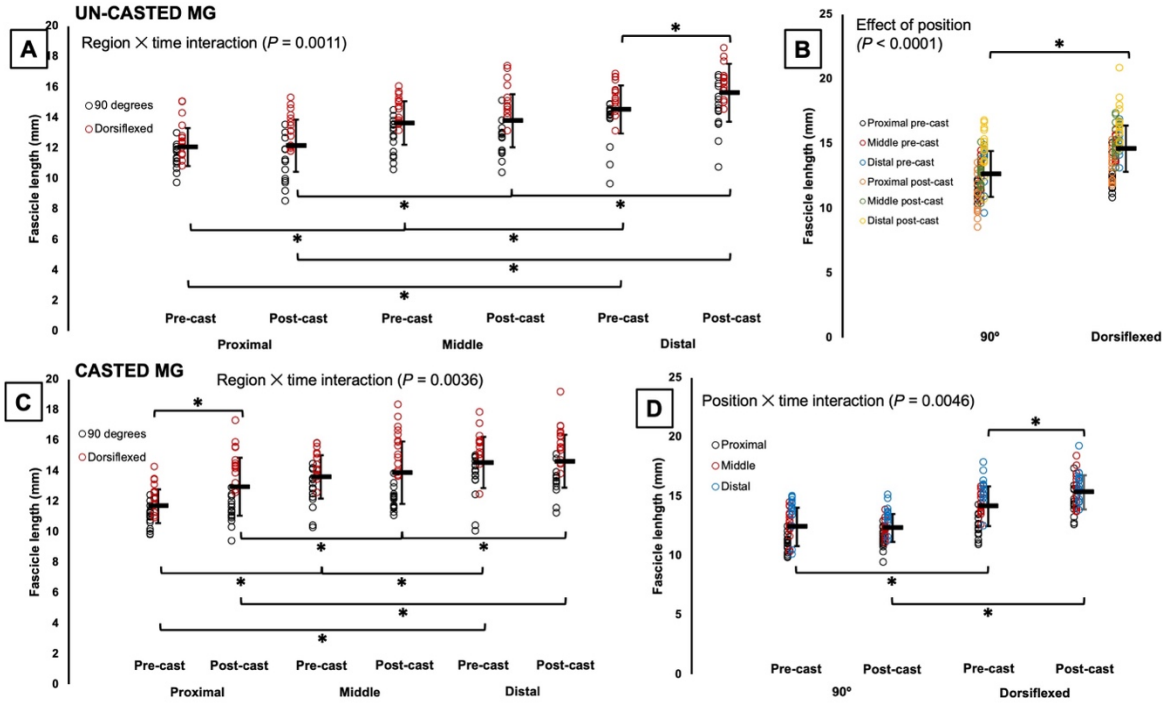

Figure 4: Fascicle length of the un-casted and casted medial gastrocnemius (MG) measured via ultrasound. For the un-casted MG, there was an interaction between region and time (A) and an effect of position (B). For the casted MG, there were interactions between region and time (C) and position and time (D). *Significant difference between indicated means (P < 0.05). Data are presented as mean ± standard deviation.

Effect of time on pennation angle measured via ultrasound

Three-way ANOVA results for PA measured via ultrasound are presented in Table 3.

For the un-casted LG, there was an effect of time (Table 3) such that PA increased by ~10% pre to post-cast (Figure 5A). For the casted LG, there was a region × joint position × time

interaction (Table 3). Pairwise comparisons showed a 26% decrease in PA pre to post-cast only in distal fascicles at full dorsiflexion ($P < 0.0001$, $d = 3.24$) (Figure 5B).

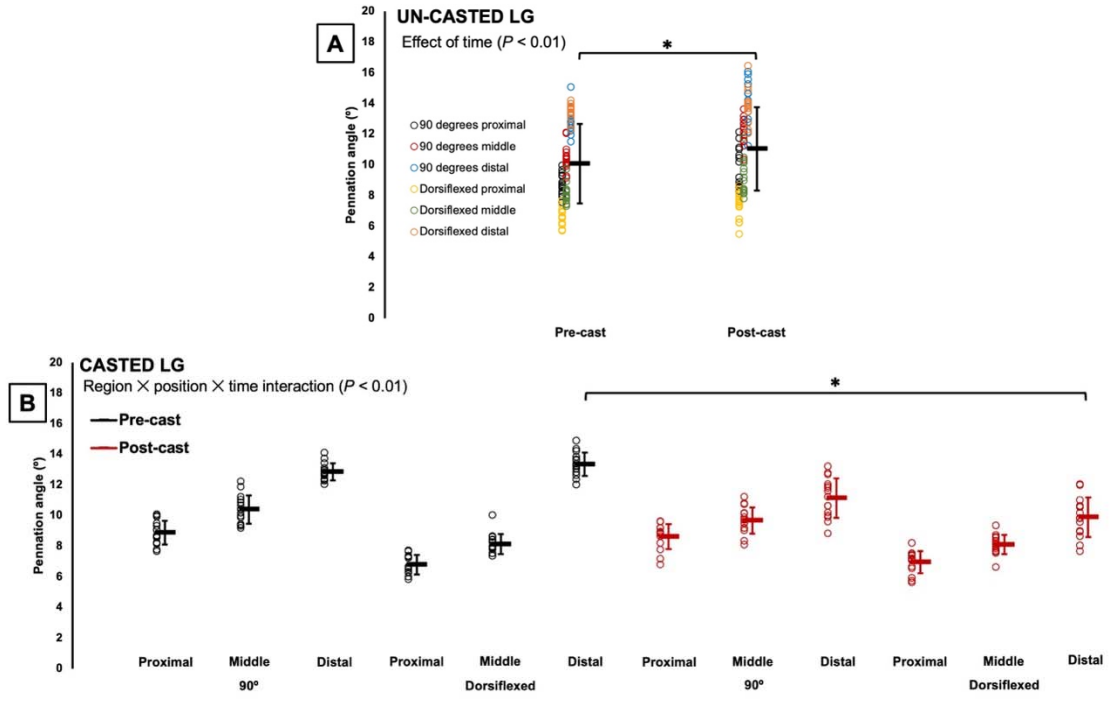

Figure 5: Changes in pennation angle of the un-casted (A) and casted (B) lateral gastrocnemius (LG) from pre to post-cast. *Significant difference between indicated means ($P < 0.05$). Data are presented as mean ± standard deviation.

For the un-casted soleus, like with FL, time did not affect PA, with no changes pre to post-cast (Table 3; Figure 6A). For the casted soleus, there were interactions of region × time and joint position × time (Table 3). Pairwise comparisons showed that at all regions of muscle, and both joint angles, PA of the casted soleus decreased (9-31%) pre to post-cast ($P < 0.0001$-0.0005, $d = 1.08$-2.78) (Figure 6B-C).

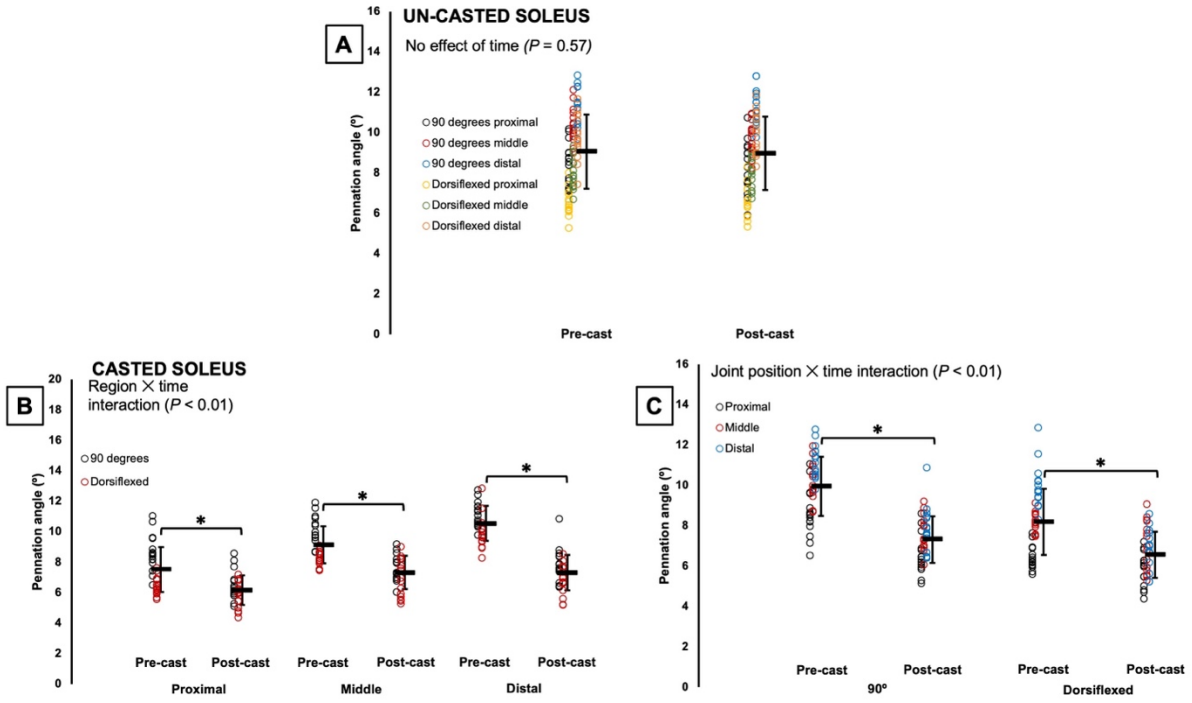

Figure 6: Changes in pennation angle of the un-casted (A) and casted (B-C) soleus from pre to post-cast. *Significant difference between indicated means ($P < 0.05$). Data are presented as mean ± standard deviation.

For the un-casted MG, time did not affect PA, with no changes pre to post-cast (Table 3; Figure 7A). For the casted MG, there was a region × time interaction (Table 3), and pairwise comparisons showed that at all three regions of the muscle, PA decreased by ~20% pre to post-cast ($P < 0.0001$-0.0003, $d = 1.10$-2.05) (Figure 7B).

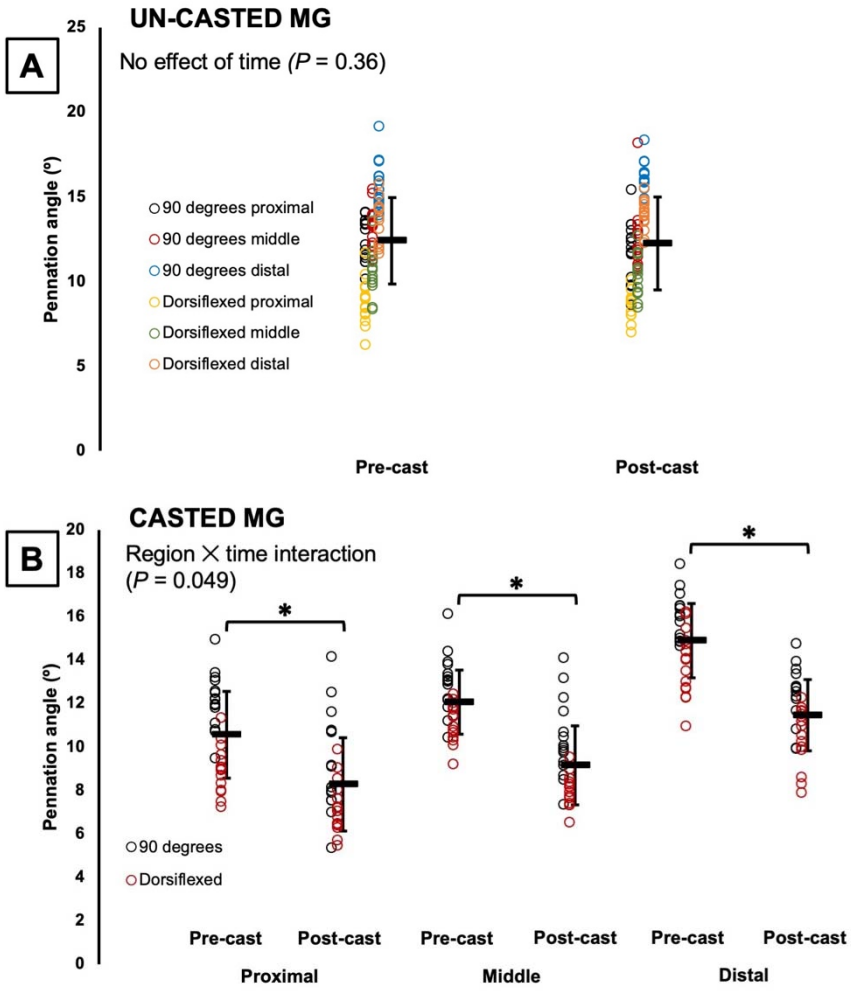

Figure 7: Changes in pennation angle of the un-casted (A) and casted (B) medial gastrocnemius (MG) from pre to post-cast. *Significant difference between indicated means ($P < 0.05$). Data are presented as mean ± standard deviation.

Muscle wet weight in the casted versus un-casted leg

The LG, soleus, and MG of the casted leg weighed 62%, 33%, and 54% less, respectively, than the muscles of the un-casted leg ($P < 0.0001$, $d = 2.42$-2.96) (Figure 8).

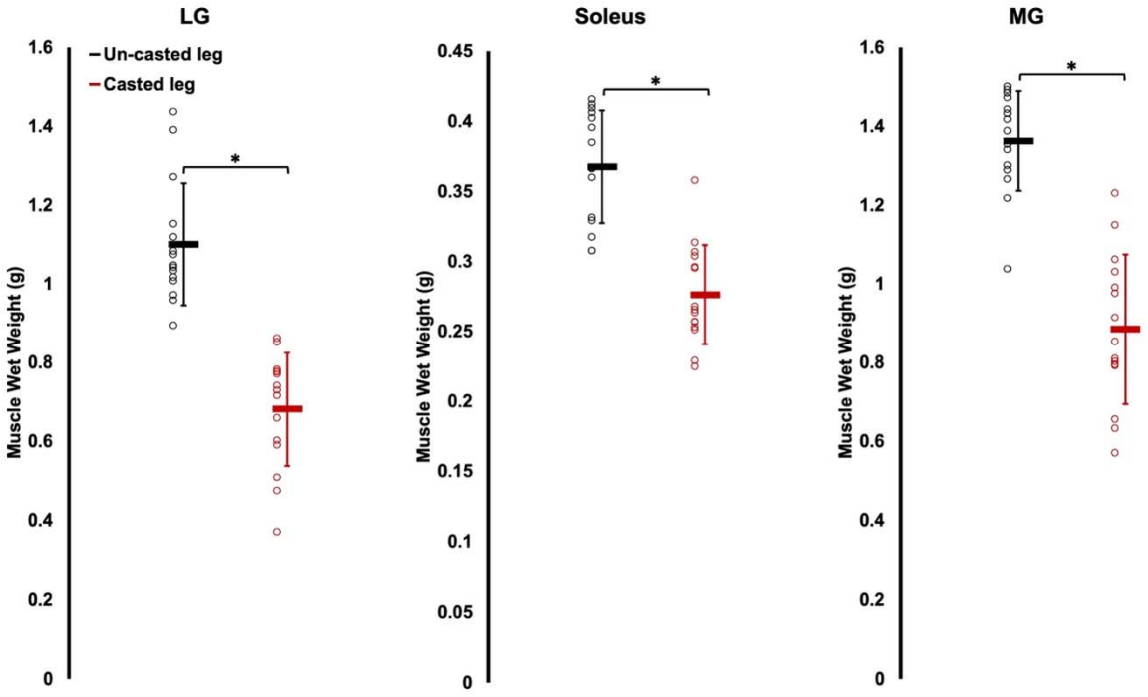

Figure 8: Comparison of muscle wet weight between the casted and un-casted leg for the lateral gastrocnemius (LG), soleus, and medial gastrocnemius (MG). *Significant difference between indicated means ($P < 0.05$). Data are presented as mean ± standard deviation.

Serial sarcomere number, sarcomere length, and fascicle length of the dissected fascicles in the casted versus non-casted leg

Two-way ANOVA results for SSN, SL, and FL of the dissected fascicles are shown in Table 4. There were no region × leg interactions for any muscles.

For the LG, there were effects of leg (Table 4) on SL and FL of dissected fascicles such that they were 3% and 6% shorter, respectively, in the casted LG (Figure 9B-C). SSN did not differ between the casted and un-casted LG (Figure 9A). There were effects of region on SSN, SL, and FL. SSN increased from proximal to middle to distal ($P < 0.0001$, $d = 1.30$-3.24) (Figure 9D), and FL followed a similar trend ($P < 0.0001$, $d = 1.58$-2.04) but with no difference between proximal and middle FL ($P = 0.0521$) (Figure 9F). Conversely, SL decreased from proximal to middle to distal ($P < 0.0001$-0.0016, $d = 0.90$-2.41) (Figure 9E).

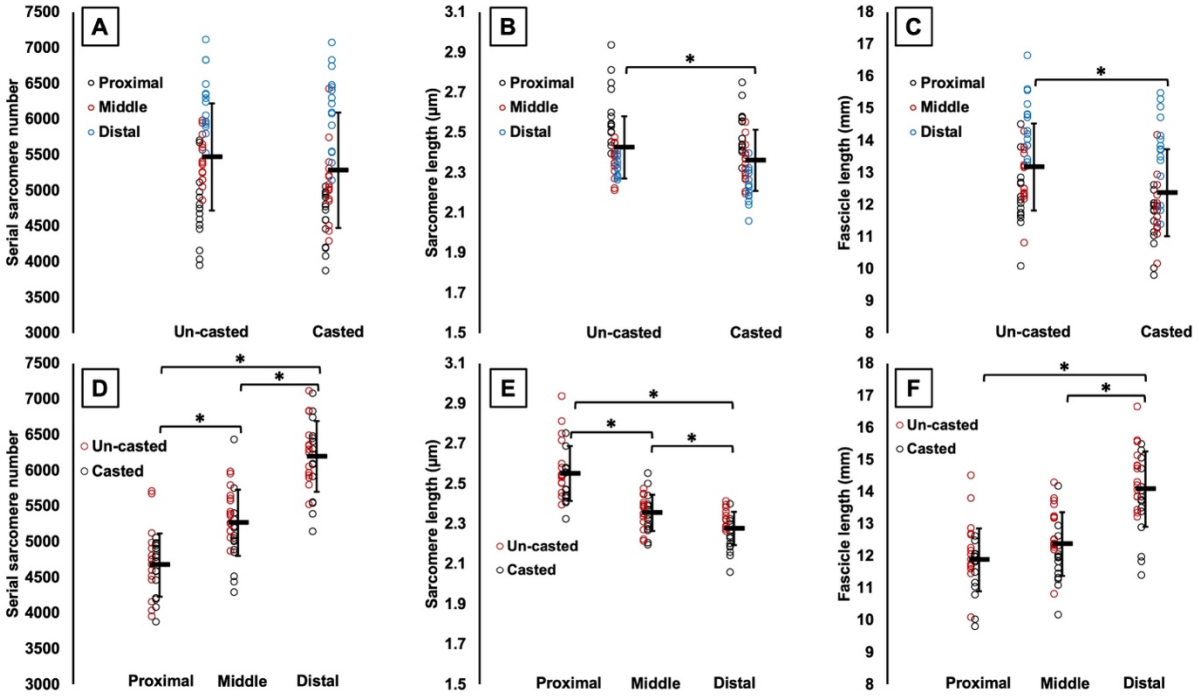

Figure 9: Effects of time (A to C) and effects of region (D to F) on serial sarcomere number (A and D), sarcomere length (B and E), and fascicle length (C and F) of the lateral gastrocnemius from dissected fascicles. *Significant difference between indicated means ($P < 0.05$). Data are presented as mean ± standard deviation.

For the soleus, there were no effects of region on SSN, SL, or dissected FL, indicating no regional differences (Table 4). There was an effect of leg on soleus SSN (Table 4) such that SSN was 6% greater in the casted leg (Figure 10A). There was a similar effect of leg on FL (Table 4), with a 6% increase (Figure 10C). Soleus SL did not differ between the casted and un-casted leg (Table 4; Figure 10B).

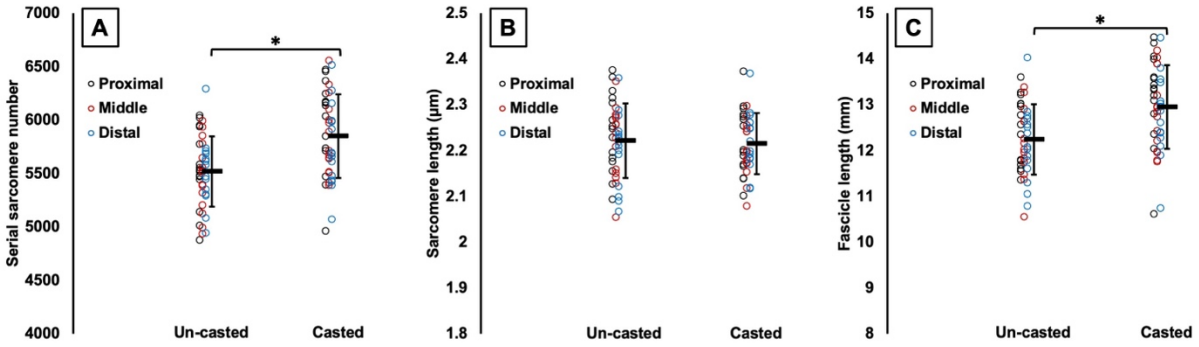

Figure 10: Effects of time on serial sarcomere number (A), sarcomere length (B), and fascicle length (C) of the soleus from dissected fascicles. *Significant difference between indicated means ($P < 0.05$). Data are presented as mean ± standard deviation.

For the MG, there were effects of leg on SL and dissected FL (Table 4) such that they were 2% and 4% shorter, respectively, in the casted MG (Figure 11B-C). SSN did not differ between the casted and un-casted MG (Figure 11A). There were effects of region on SSN, SL, and FL (Table 4). SSN followed the same pattern as in the LG, increasing from proximal to middle to distal ($P < 0.0001$-0.0127, $d = 0.79$-1.42) (Figure 11D). FL only differed between proximal and distal fascicles, with distal fascicles being longer ($P = 0.0044$, $d = 0.43$) (Figure 11F). Like with the LG, SL decreased from proximal to middle to distal ($P < 0.0001$-0.0481, $d = 0.52$-1.49) (Figure 11E).

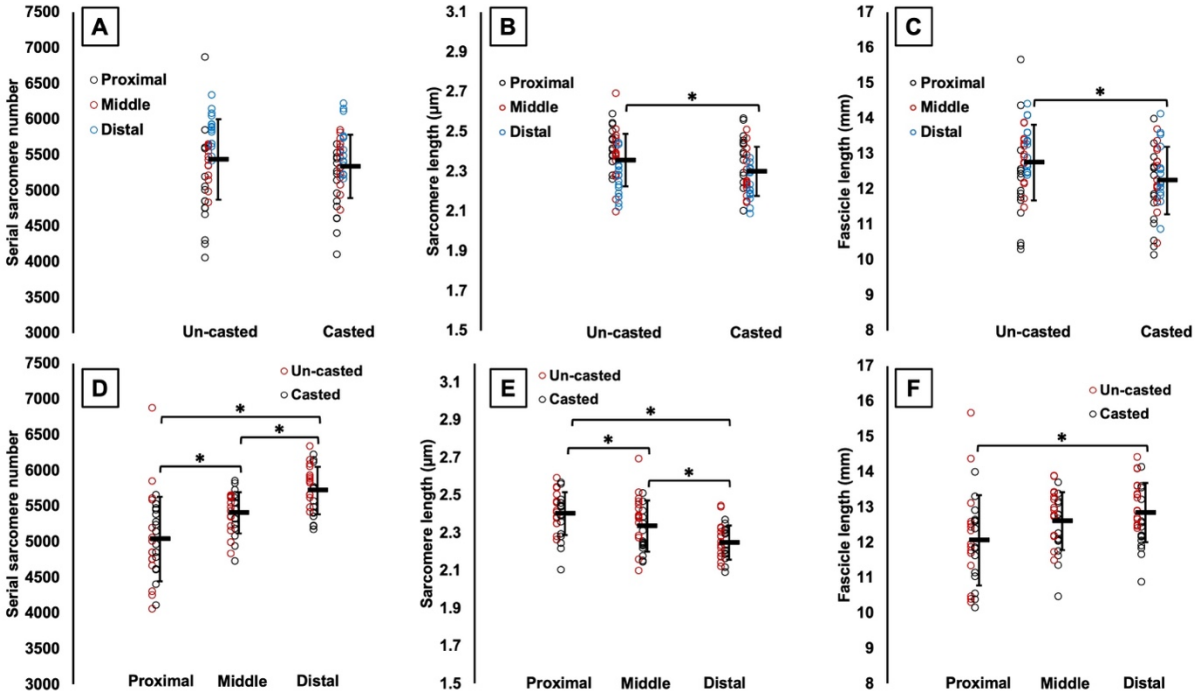

Figure 11: Effects of time (A to C) and effects of region (D to F) on serial sarcomere number (A and D), sarcomere length (B and E), and fascicle length (C and F) of the medial gastrocnemius from dissected fascicles. *Significant difference between indicated means ($P < 0.05$). Data are presented as mean ± standard deviation.

Relationships between adaptations in fascicle length measured via ultrasound and adaptations in serial sarcomere number and fascicle length measured from dissected fascicles

For the soleus, significant positive relationships were found between ultrasound-derived FL at 90° and FL of dissected fascicles (Figure 12A) and SSN (Figure 12D), and between ultrasound-derived FL at full dorsiflexion and SSN (Figure 12G). For the LG, there was only a relationship between ultrasound-derived FL at 90° and FL of dissected fascicles (Figure 12B), and no relationships among these measures were observed for the MG (Figure 12C, F, I).

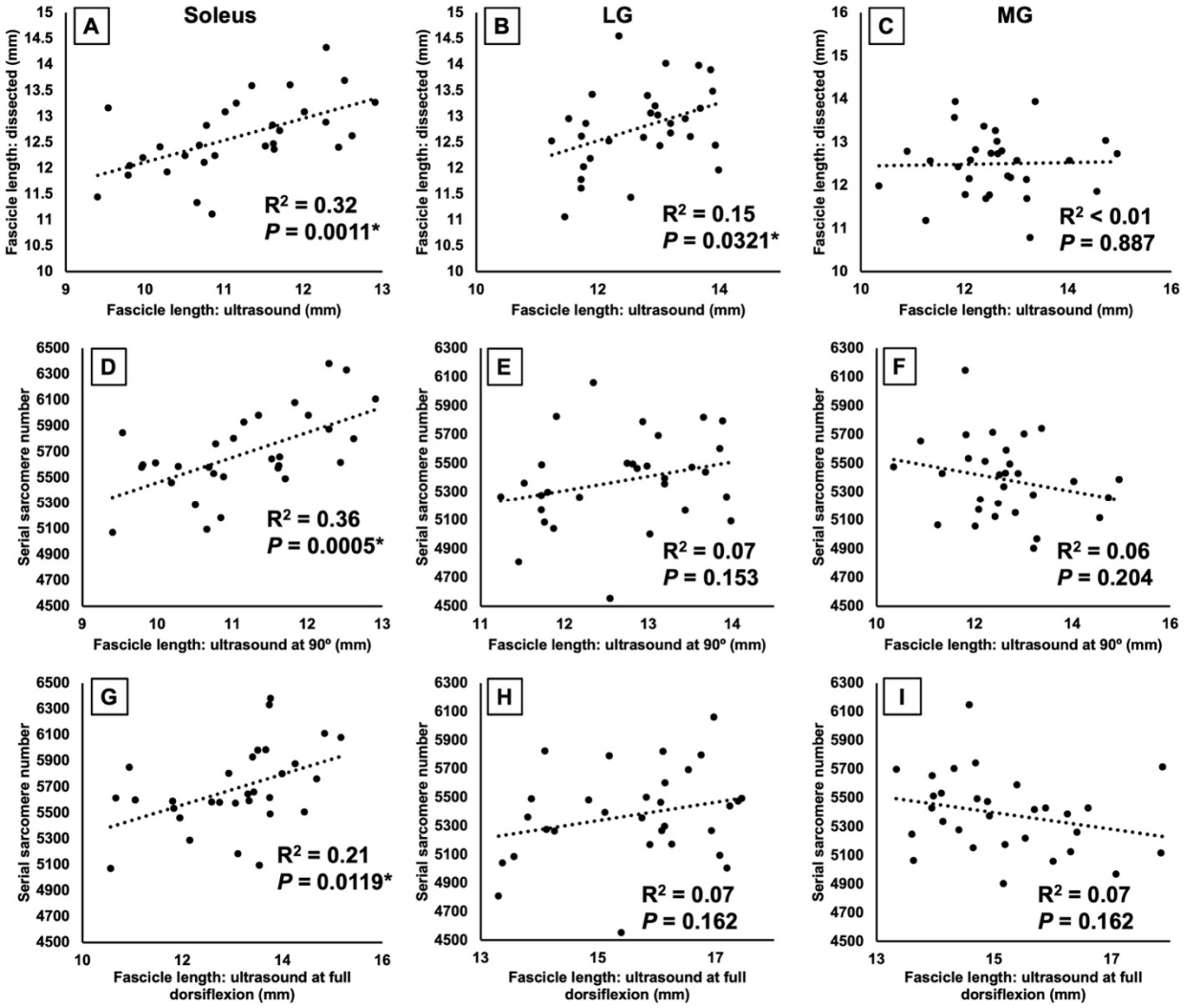

Figure 12: Relationships between ultrasound-derived fascicle length at 90° and fascicle length of dissected fascicles (A-C), ultrasound-derived fascicle length at 90° and SSN (D-F), and ultrasound-derived FL at full dorsiflexion and SSN (G-I) for the soleus, lateral gastrocnemius (LG), medial gastrocnemius (MG). *Significant relationship ($P < 0.05$).

There were no relationships between the % change in ultrasound-derived FL from pre to post-cast and the % change in SSN from the un-casted to casted leg for the LG, soleus, or MG (Table 5).

When regression analyses were performed across all muscles together, the % change in ultrasound-derived FL measured with the ankle at 90° explained 28% of the variation in the %

367 change in SSN from dissected fascicles (Figure 13A). This relationship was lessened when using
368 ultrasound-derived FL at full dorsiflexion, only explaining 10% of the variation in SSN
369 adaptations (Figure 13B).

370

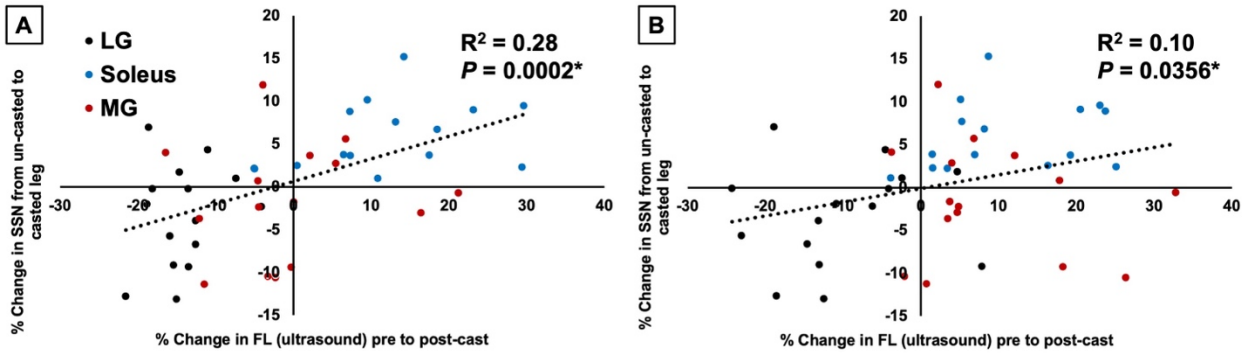

371

372 **Figure 13:** For all muscles combined, relationships between the % change in ultrasound-derived
373 fascicle length (FL) from pre to post-cast as measured with the ankle at 90° (A) and full
374 dorsiflexion (B) and the % change in serial sarcomere number (SSN) from the un-casted to
375 casted leg determined from dissected fascicles. *Significant relationship ($P < 0.05$).

Table 2: Three-way ANOVA results for ultrasound-derived fascicle length

		Effect of region		Effect of joint position		Effect of time		Region × joint position interaction		Region × time interaction		Joint position × time interaction		Region × joint position × time interaction	
		F	***P***	**F**	***P***	**F**	***P***	**F**	***P***	**F**	***P***	**F**	***P***	**F**	***P***
LG	**Un-casted**	393.80	**<0.0001***	215.10	**<0.0001***	3.99	0.0819	3.01	0.0655	0.08	0.921	17.79	**0.0014***	0.01	0.970
	Casted	271.00	**<0.0001***	269.10	**<0.0001***	50.10	**<0.0001***	2.43	0.106	3.02	0.0649	0.60	0.414	3.08	0.0954
Soleus	**Un-casted**	10.49	**0.0022***	148.90	**<0.0001***	0.09	0.677	3.39	**0.0480***	2.07	0.145	1.13	0.296	0.67	0.426
	Casted	24.83	**<0.0001***	236.80	**<0.0001***	27.64	**0.0003***	0.15	0.861	10.57	**0.0004***	0.17	0.662	0.26	0.629
MG	**Un-casted**	101.20	**<0.0001***	99.57	**<0.0001***	1.43	0.240	1.39	0.266	8.75	**0.0011***	2.70	0.132	1.69	0.214
	Casted	120.30	**<0.0001***	159.80	**<0.0001***	3.62	0.0844	1.03	0.369	6.91	**0.0036***	14.30	**0.0046***	4.13	0.0596

Table 3: Three-way ANOVA results for ultrasound-derived pennation angle

		Effect of region		Effect of joint position		Effect of time		Region × joint position interaction		Region × time interaction		Joint position × time interaction		Region × joint position × time interaction	
		F	***P***	**F**	***P***	**F**	***P***	**F**	***P***	**F**	***P***	**F**	***P***	**F**	***P***
LG	**Un-casted**	371.09	**<0.0001***	101.59	**<0.0001***	69.40	**<0.0001***	44.15	**<0.0001***	2.32	0.117	2.69	0.126	0.43	0.568
	Casted	274.65	**<0.0001***	147.66	**<0.0001***	55.73	**<0.0001***	35.91	**<0.0001***	32.54	**<0.0001***	0.63	0.391	12.81	**0.0013***
Soleus	**Un-casted**	245.15	**<0.0001***	163.54	**<0.0001***	0.24	0.570	4.02	**0.0292***	1.18	0.321	1.16	0.285	0.46	0.543
	Casted	73.30	**<0.0001***	85.29	**<0.0001***	122.94	**<0.0001***	1.05	0.362	20.55	**<0.0001***	20.29	**0.0009***	2.28	0.144
MG	**Un-casted**	132.70	**<0.0001***	140.88	**<0.0001***	0.81	0.357	4.51	**0.0201***	3.13	0.0593	1.37	0.260	0.11	0.767
	Casted	139.24	**<0.0001***	182.18	**<0.0001***	80.12	**<0.0001***	2.02	0.152	3.34	**0.0499***	0.20	0.634	1.28	0.278

Table 4: Two-way ANOVA results for serial sarcomere number, sarcomere length, and fascicle length of dissected fascicles

		Effect of region		Effect of leg		Region × leg interaction	
		F	***P***	**F**	***P***	**F**	***P***
LG	**SSN**	108.91	**<0.0001***	4.57	0.0507	0.67	0.502
	SL	61.46	**<0.0001***	8.37	**0.0118***	2.77	0.0959
	FL	55.00	**<0.0001***	11.57	**0.0043***	0.17	0.793
Soleus	**SSN**	1.39	0.267	33.02	**<0.0001***	0.68	0.475
	SL	1.26	0.291	0.14	0.713	0.64	0.514
	FL	3.06	0.0639	22.94	**0.0003***	0.10	0.871
MG	**SSN**	21.30	**<0.0001***	0.99	0.336	1.01	0.374
	SL	18.36	**<0.0001***	6.27	**0.0253***	1.02	0.373
	FL	7.77	**0.0111***	5.03	**0.0416***	0.62	0.541

Table 5: Relationships between % change in ultrasound-derived fascicle length (FL) from pre to post-cast and % change in serial sarcomere number of dissected fascicles from the un-casted to casted leg

		Ultrasound-derived FL at 90°		Ultrasound-derived FL at full dorsiflexion	
		R^2	***P***	**R^2**	***P***
Serial Sarcomere Number	**LG**	0.04	0.462	0.02	0.659
	Soleus	0.13	0.180	0.06	0.381
	MG	0.01	0.666	0.03	0.547

LG = lateral gastrocnemius; MG = medial gastrocnemius

Discussion

Immobilizing the rat ankle in full dorsiflexion for 2 weeks, the present study investigated whether ultrasound-derived FL measurements can accurately depict SSN adaptations. Ultrasound detected an 11% increase in soleus FL, a 12% decrease in LG FL, and (depending on the joint angle and region of muscle) an 8% increase in MG FL. These adaptations were partly reflected by the SSN measurements obtained from dissected fascicles, with a 6% greater soleus SSN in the casted leg than the un-casted leg, but no differences in SSN for the gastrocnemii. Our results indicate that ultrasonographic measurements of FL can overestimate SSN adaptations.

Our values for muscle wet weight, SSN, SL, FL, and ultrasound-derived PA are within previously reported ranges for the rat soleus (Booth, 1977; Soares *et al.*, 2007; Peixinho *et al.*, 2011; Mele *et al.*, 2016; Chen *et al.*, 2020; Hinks *et al.*, 2022*b*) and gastrocnemii (Booth, 1977; Woittiez *et al.*, 1986; Ochi *et al.*, 2007; Peixinho *et al.*, 2011; Mele *et al.*, 2016; Power *et al.*, 2021).

Stretch-induced adaptation in serial sarcomere number

The soleus of the casted leg had a 6% greater SSN than the un-casted leg, which is consistent with findings from previous studies that immobilized the soleus in a stretched position in rats, mice, and cats (Tabary *et al.*, 1972; Williams & Goldspink, 1978; Spector *et al.*, 1982; Shah *et al.*, 2001; Soares *et al.*, 2007; Kinney *et al.*, 2017). This serial sarcomere addition is believed to occur to restore optimal actin-myosin overlap and reduce sarcomeric passive tension in the stretched position (Williams & Goldspink, 1978; Davis *et al.*, 2020; Hinks *et al.*, 2022*a*). The increase in rat soleus SSN we observed after 2 weeks of immobilization was notably lower (+6%, from 5518 to 5850 sarcomeres) than the increase reported by Soares *et al.* (2007) after

immobilizing the soleus in a stretched position for just 4 days (+29%, 6338 to 8174 sarcomeres). This discrepancy may be attributed to the more extreme ankle angle they used for immobilization, described as "total dorsiflexion," while we immobilized the ankle at 40°. Additionally, we did not observe a difference in SSN between the casted and un-casted legs for the gastrocnemii. The gastrocnemii are biarticular muscles, crossing the ankle and the knee. Spector *et al.* (1982) immobilized the knee in full extension and the ankle at 45°, and observed a 20% increase in MG SSN. While we immobilized the ankle at a similar angle (40°), we did not immobilize the knee, allowing movement of the gastrocnemii at that joint, which likely tempered the stretch stimulus imposed by dorsiflexion for those muscles.

Immobilization-induced atrophy

Our casting intervention induced atrophy in the gastrocnemii and soleus, as evidenced by lower muscle wet weights in the casted leg. Measurements of PA provided by ultrasound align with these findings, showing decreased PA from pre to post-cast in all three muscles, which may reflect the loss of sarcomeres in parallel (Wisdom *et al.*, 2015; Jorgenson *et al.*, 2020). The reduced muscle weight was more pronounced in the gastrocnemii (–54-62%) than the soleus (–33%). Considering the soleus had a 6% greater SSN in the casted than the un-casted leg, an increase in SSN due to stretch may have lessened the overall loss of muscle tissue, limiting the loss to only sarcomeres in parallel. A similar result was observed by Spector *et al.* (1982), with a smaller reduction in soleus wet weight when immobilizing in a stretched position (–14%) than a shortened position (–48%), and the former increasing SSN while the latter decreased SSN. The gastrocnemii in the present study did not appear to experience an increase in SSN, therefore, the

loss of parallel sarcomeres may not have been made up for by stretch-induced serial sarcomere addition, resulting in a greater loss of muscle weight.

Can the un-casted leg be used as a valid control?

In the un-casted soleus, no differences in FL or PA were detected by ultrasound from pre to post-cast, validating the use of the un-casted soleus as a SSN control in the present study and previous studies (Williams & Goldspink, 1978; Heslinga & Huijing, 1993; Shah *et al.*, 2001; Gomes *et al.*, 2004; Kinney *et al.*, 2017). In the un-casted gastrocnemii, however, ultrasound measurements suggest some adaptations may have occurred, possibly due to the un-casted leg compensating for the added load (the cast) on the opposite leg during ambulation. In the un-casted LG, ultrasound showed a 6% decrease in FL at 90°, accompanied by a 10% increase in PA. Increased PA and sometimes a decrease in FL are often observed following training emphasizing concentric contractions, and may reflect a reorganization of the muscle architecture to add sarcomeres in parallel for greater force production (Butterfield *et al.*, 2005; Franchi *et al.*, 2014).

Ultrasound-derived FL does not perfectly reflect adaptations in serial sarcomere number

Measurements of FL via ultrasound are often used to infer increases or decreases in SSN (Narici *et al.*, 2003; Blazevich *et al.*, 2007; Franchi *et al.*, 2014; Hinks *et al.*, 2021). Inferring SSN adaptations from ultrasound-derived FL may be problematic, however, because apparent changes in FL may simply be due to changes in SL at the joint angle at which ultrasound measurements are obtained. For example, Pincheira *et al.* (2021) observed an increase in biceps femoris FL following 3 weeks of eccentric training as measured with the leg in full extension;

453 however, microendoscopy revealed the increase in FL was only due to longer SLs at that joint
454 angle, not training-induced serial sarcomere addition. In research on animals, SSN adaptations
455 are often determined by calculating SSN from measurements of SL and FL from dissected
456 fascicles, then comparing between experimental and control muscles. The present study
457 investigated the relationship between these two most commonly used methodologies for
458 assessing SSN adaptations.

459 We observed significant but weak relationships between ultrasound-derived FL at 90°
460 and FL of dissected fascicles (after being fixed at 90°) for the soleus and LG (Figure 12A-B).
461 *Kellis et al.* (2009) observed moderate to strong relationships between FL measured via
462 ultrasound and FL measured directly in the hamstrings of human cadavers. Our results may
463 differ from theirs because, after digesting the muscles in nitric acid, it was more difficult to
464 ensure that the same fascicles as the ultrasound images were being measured from the dissected
465 muscle, even though the same regional constraints (two fascicles from each of the proximal,
466 middle, and distal regions) were followed. Additionally, we observed relationships between
467 ultrasound-derived measurements of FL and actual SSN determined from dissected fascicles for
468 the soleus only, and between the % change in FL from pre to post-cast and the % change in SSN
469 from the un-casted to casted leg with all muscles together. In both cases, the relationships using
470 FL measured at full dorsiflexion were weaker than when using FL measured at 90°. Similar
471 findings were observed recently by Werkhausen *et al.* (2023), with the relationship between
472 ultrasound-derived FL and isokinetic force (i.e., a measure associated with SSN (Drazan *et al.*,
473 2019; Hinks *et al.*, 2022*a*)) being moderate or non-existent depending on the joint angle used
474 during ultrasound imaging. Collectively, our regression analyses demonstrate variability both

among muscles and between joint angles in the ability for ultrasound-derived FL to truly represent SSN.

Overall, the soleus provided the best means for comparing ultrasound-derived FL adaptations and adaptations in SSN, as the un-casted soleus did not appear to undergo any compensatory adaptations. From the ultrasound measurements, we observed an ~11% increase in soleus FL from pre to post-cast, however, the true increase in SSN from the un-casted to the casted leg was only 6%. This serial sarcomere addition appeared to be driven by a 6% increase in FL, as the un-casted and casted soleus had the same SL (~2.2 μm) with the ankle fixed at 90°. Interestingly, while ultrasound-derived FL averaged across muscle regions increased by 11%, the increase in ultrasound-derived FL of proximal fascicles (+6%) was closer to the observed increase in SSN, demonstrating regional variability in the accuracy of ultrasound-derived FL measurements. Altogether, an increase in FL measured by ultrasound can indeed correspond to an increase in SSN in the rat soleus, but may overestimate the increase in SSN by as much as 5%.

Limitations of ultrasound that may contribute to a disconnect between ultrasound-derived FL and actual SSN

For the gastrocnemii, the distal fascicles were sometimes partly out of plane (Figure 1), thus the trajectory of those fascicles to the deep aponeurosis was used to complete the measurements of FL. This limitation likely contributed to the higher coefficients of variation for the gastrocnemii compared to the soleus (Table 1), and may explain the lack of relationships observed between ultrasound-derived FL and dissected FL and SSN for the gastrocnemii, but not the soleus. It is also important to note that ultrasound images do not capture the contractile tissue

498 of muscle fascicles, but rather the perimysium, the sheath of connective tissue surrounding each
499 fascicle. During serial sarcomerogenesis, the connective tissue scaffolding must be constructed
500 before sarcomeres are added within that space (Kjær, 2004). Previous studies have reported no
501 changes (Williams *et al.*, 1988) or increases in intramuscular connective tissue content
502 (Ahtikoski *et al.*, 2001) following immobilization in a stretched position depending on the
503 duration of immobilization. Many studies also overlook that adaptations in connective tissue
504 structure (e.g., crosslinking, collagen fibril orientation, organization) may not be evident in
505 measures of only content, but can change during muscle remodelling as well (Kjær, 2004).
506 Connective tissue is digested in nitric acid before measurements are performed on dissected
507 fascicles, therefore, variability in connective tissue likely affects the ability for ultrasound to
508 capture FL of only contractile tissue. Furthermore, an ultrasound image only captures a fascicle
509 path in two dimensions, but the three-dimensional nature of fascicle curvature is well-
510 documented (Rana *et al.*, 2013; Raiteri *et al.*, 2016; Cameron *et al.*, 2023). Unless methods such
511 as three-dimensional ultrasound (Raiteri *et al.*, 2016) or magnetic resonance diffusion tensor
512 imaging (Cameron *et al.*, 2023) are used, the three-dimensional nature of FL can only be
513 accounted for when fascicles are dissected out of the muscle. In the present study, this two-
514 dimensional limitation of ultrasound is most evident in how dissected FLs of the soleus were
515 ~13% longer than ultrasound-derived FLs. There may be curvature in rat soleus fascicles that is
516 not captured in a lateral ultrasound scan, making fascicles appear shorter. Altogether, these
517 factors may have contributed to the disconnects between ultrasound-derived FL and actual SSN
518 in the present study, including the ~5% overestimation of sarcomerogenesis in the soleus, and
519 should be considered going forward in studies employing muscle ultrasound.
520

Conclusion

The present study investigated the relationship between the two most commonly used methods of assessing longitudinal growth of skeletal muscle: 1) ultrasound-derived FL measurements pre and post-intervention; and 2) comparison of SSN between an experimental and a control muscle. We showed that ultrasound-derived FL overestimated SSN adaptations by ~5%, with measurements in a neutral position predicting SSN better than measurements in a stretched position. Future studies should consider these findings when concluding a large magnitude of serial sarcomerogenesis based on ultrasound-derived FL taken at a set joint angle, and may consider applying a correction factor to more closely approximate the actual SSN adaptations.

Acknowledgements

This project was supported by the Natural Sciences and Engineering Research Council of Canada (NSERC). No conflicts of interest, financial or otherwise, are declared by the authors.

Conflict of interest statement

No conflicts of interest, financial or otherwise, are declared by the authors.

Ethics statement

Approval was given by the University of Guelph's Animal Care Committee and all protocols followed CCAC guidelines (AUP #4905).

Data accessibility

Individual values of all supporting data are available upon request.

Grants

This project was supported by the Natural Sciences and Engineering Research Council of Canada (NSERC), grant number RGPIN-2017-06012.

Author contributions

A.H., M.V.F. and G.A.P. conceived and designed research; A.H. carried out animal husbandry and training; A.H. performed experiments; A.H. analyzed data; A.H., M.V.F., and G.A.P. interpreted results of experiments; A.H. prepared figures; A.H. and G.A.P. drafted manuscript; A.H., M.V.F., and G.A.P. edited and revised manuscript; A.H., M.V.F., and G.A.P. approved final version of manuscript.

References

Adkins AN, Dewald JPA, Garmirian LP, Nelson CM & Murray WM (2021). Serial sarcomere number is substantially decreased within the paretic biceps brachii in individuals with chronic hemiparetic stroke. *Proc Natl Acad Sci* **118,** e2008597118.

Ahtikoski AM, Koskinen SOA, Virtanen P, Kovanen V & Takala TES (2001). Regulation of synthesis of fibrillar collagens in rat skeletal muscle during immobilization in shortened and lengthened positions. *Acta Physiol Scand* **172,** 131–140.

Aoki MS, Soares AG, Miyabara EH, Baptista IL & Moriscot AS (2009). Expression of genes related to myostatin signaling during rat skeletal muscle longitudinal growth: Myostatin and Longitudinal Growth. *Muscle Nerve* **40,** 992–999.

Blazevich AJ, Cannavan D, Coleman DR & Horne S (2007). Influence of concentric and eccentric resistance training on architectural adaptation in human quadriceps muscles. *J Appl Physiol* **103,** 1565–1575.

Boakes JL, Foran J, Ward SR & Lieber RL (2007). Muscle adaptation by serial sarcomere addition 1 year after femoral lengthening. *Clin Orthop* **456,** 250–253.

de Boer MD, Seynnes OR, di Prampero PE, Pišot R, Mekjavić IB, Biolo G & Narici MV (2008). Effect of 5 weeks horizontal bed rest on human muscle thickness and architecture of weight bearing and non-weight bearing muscles. *Eur J Appl Physiol* **104,** 401–407.

Booth FW (1977). Time course of muscular atrophy during immobilization of hindlimbs in rats. *J Appl Physiol* **43,** 656–661.

Butterfield TA, Leonard TR & Herzog W (2005). Differential serial sarcomere number adaptations in knee extensor muscles of rats is contraction type dependent. *J Appl Physiol* **99,** 7.

Cameron D, Reiter DA, Adelnia F, Ubaida-Mohien C, Bergeron CM, Choi S, Fishbein KW, Spencer RG & Ferrucci L (2023). Age-related changes in human skeletal muscle microstructure and architecture assessed by diffusion-tensor magnetic resonance imaging and their association with muscle strength. *Aging Cell*e13851.

Chen J, Mashouri P, Fontyn S, Valvano M, Elliott-Mohamed S, Noonan AM, Brown SHM & Power GA (2020). The influence of training-induced sarcomerogenesis on the history dependence of force. *J Exp Biol* **223,** jeb218776.

Davis JF, Khir AW, Barber L, Reeves ND, Khan T, DeLuca M & Mohagheghi AA (2020). The mechanisms of adaptation for muscle fascicle length changes with exercise: Implications for spastic muscle. *Med Hypotheses* **144,** 110199.

Drazan JF, Hullfish TJ & Baxter JR (2019). Muscle structure governs joint function: linking natural variation in medial gastrocnemius structure with isokinetic plantar flexor function. *Biol Open* **8,** bio.048520.

598 Franchi MV, Atherton PJ, Reeves ND, Flück M, Williams J, Mitchell WK, Selby A, Beltran
599 Valls RM & Narici MV (2014). Architectural, functional and molecular responses to
600 concentric and eccentric loading in human skeletal muscle. *Acta Physiol* **210,** 642–654.

601 Franchi MV, Fitze DP, Raiteri BJ, Hahn D & Spörri J (2020). Ultrasound-derived Biceps
602 Femoris Long Head Fascicle Length: Extrapolation Pitfalls. *Med Sci Sports Exerc* **52,**
603 233–243.

604 Gomes ARS, Coutinho EL, França CN, Polonio J & Salvini TF (2004). Effect of one stretch a
605 week applied to the immobilized soleus muscle on rat muscle fiber morphology. *Braz J*
606 *Med Biol Res* **37,** 1473–1480.

607 Heslinga JW & Huijing PA (1993). Muscle length-force characteristics in relation to muscle
608 architecture: a bilateral study of gastrocnemius medialis muscles of unilaterally
609 immobilized rats. *Eur J Appl Physiol* **66,** 289–298.

610 Hinks A, Davidson B, Akagi R & Power GA (2021). Influence of isometric training at short and
611 long muscle-tendon unit lengths on the history dependence of force. *Scand J Med Sci*
612 *Sports* **31,** 325–338.

613 Hinks A, Franchi MV & Power GA (2022*a*). The influence of longitudinal muscle fascicle
614 growth on mechanical function. *J Appl Physiol* **133,** 87–103.

615 Hinks A, Jacob K, Mashouri P, Medak KD, Franchi MV, Wright DC, Brown SHM & Power GA
616 (2022*b*). Influence of weighted downhill running training on serial sarcomere number and
617 work loop performance in the rat soleus. *Biol Open* **11,** bio059491.

618 Jorgenson KW, Phillips SM & Hornberger TA (2020). Identifying the Structural Adaptations
619 that Drive the Mechanical Load-Induced Growth of Skeletal Muscle: A Scoping Review.
620 *Cells* **9,** 1658.

621 Kellis E, Galanis N, Natsis K & Kapetanos G (2009). Validity of architectural properties of the
622 hamstring muscles: Correlation of ultrasound findings with cadaveric dissection. *J*
623 *Biomech* **42,** 2549–2554.

624 Kinney MC, Dayanidhi S, Dykstra PB, McCarthy JJ, Peterson CA & Lieber RL (2017). Reduced
625 skeletal muscle satellite cell number alters muscle morphology after chronic stretch but
626 allows limited serial sarcomere addition: Satellite Cells and Sarcomere Addition. *Muscle*
627 *Nerve* **55,** 384–392.

628 Kjær M (2004). Role of Extracellular Matrix in Adaptation of Tendon and Skeletal Muscle to
629 Mechanical Loading. *Physiol Rev* **84,** 649–698.

630 Lichtwark GA, Farris DJ, Chen X, Hodges PW & Delp SL (2018). Microendoscopy reveals
631 positive correlation in multiscale length changes and variable sarcomere lengths across
632 different regions of human muscle. *J Appl Physiol* **125,** 1812–1820.

633 Lieber RL & Fridén J (2000). Functional and clinical significance of skeletal muscle
634 architecture. *Muscle Nerve* **23,** 1647–1666.

635 Lieber RL, Ljung BO & Fridén J (1997). Intraoperative sarcomere length measurements reveal
636 differential design of human wrist extensor muscles. *J Exp Biol* **200,** 19–25.

637 Lieber RL, Yeh Y & Baskin RJ (1984). Sarcomere length determination using laser diffraction.
638 Effect of beam and fiber diameter. *Biophys J* **45,** 1007–1016.

639 Mele A, Fonzino A, Rana F, Camerino GM, De Bellis M, Conte E, Giustino A, Conte Camerino
640 D & Desaphy J-F (2016). In vivo longitudinal study of rodent skeletal muscle atrophy
641 using ultrasonography. *Sci Rep* **6,** 20061.

642 Narici M, Franchi M & Maganaris C (2016). Muscle structural assembly and functional
643 consequences. *J Exp Biol* **219,** 276–284.

644 Narici MV, Maganaris CN, Reeves ND & Capodaglio P (2003). Effect of aging on human
645 muscle architecture. *J Appl Physiol* **95,** 2229–2234.

646 Ochi E, Nakazato K & Ishii N (2007). Effects of Eccentric Exercise on Joint Stiffness and
647 Muscle Connectin (Titin) Isoform in the Rat Hindlimb. *J Physiol Sci* **57,** 1–6.

648 Peixinho CC, Martins NSF, de Oliveira LF & Machado JC (2014). Structural adaptations of rat
649 lateral gastrocnemius muscle–tendon complex to a chronic stretching program and their
650 quantification based on ultrasound biomicroscopy and optical microscopic images. *Clin*
651 *Biomech* **29,** 57–62.

652 Peixinho CC, Ribeiro MB, Resende CMC, Werneck-de-Castro JPS, de Oliveira LF & Machado
653 JC (2011). Ultrasound biomicroscopy for biomechanical characterization of healthy and
654 injured triceps surae of rats. *J Exp Biol* **214,** 3880–3886.

655 Pincheira PA, Boswell MA, Franchi MV, Delp SL & Lichtwark GA (2021). Biceps femoris long
656 head sarcomere and fascicle length adaptations after three weeks of eccentric exercise
657 training. *J Sport Health Sci* **11,** 43–49.

658 Power GA, Crooks S, Fletcher JR, Macintosh BR & Herzog W (2021). Age-related reductions in
659 the number of serial sarcomeres contribute to shorter fascicle lengths but not elevated
660 passive tension. *J Exp Biol* **224,** jeb242172.

661 Power GA, Makrakos DP, Rice CL & Vandervoort AA (2013). Enhanced force production in old
662 age is not a far stretch: an investigation of residual force enhancement and muscle
663 architecture. *Physiol Rep* **1,** e00004.

664 Raiteri BJ, Cresswell AG & Lichtwark GA (2016). Three-dimensional geometrical changes of
665 the human tibialis anterior muscle and its central aponeurosis measured with three-
666 dimensional ultrasound during isometric contractions. *PeerJ* **4,** e2260.

667 Rana M, Hamarneh G & Wakeling JM (2013). 3D fascicle orientations in triceps surae. *J Appl*
668 *Physiol* **115,** 116–125.

669 Shah SB, Peters D, Jordan KA, Milner DJ, Fridén J, Capetanaki Y & Lieber RL (2001).
670 Sarcomere number regulation maintained after immobilization in desmin-null mouse
671 skeletal muscle. *J Exp Biol* **204,** 1703–1710.

672 Soares AG, Aoki MS, Miyabara EH, DeLuca CV, Ono HY, Gomes MD & Moriscot AS (2007).
673 Ubiquitin-ligase and deubiquitinating gene expression in stretched rat skeletal muscle.
674 *Muscle Nerve* **36,** 685–693.

675 Spector SA, Simard CP, Fournier M, Sternlicht E & Edgerton' VR (1982). Architectural
676 Alterations of Rat Hind-Limb Skeletal Muscles Immobilized at Different Lengths. *Exp*
677 *Neurol* **76,** 94–110.

678 Tabary JC, Tabary C, Tardieu C, Tardieu G & Goldspink G (1972). Physiological and structural
679 changes in the cat's soleus muscle due to immobilization at different lengths by plaster
680 casts. *J Physiol* **224,** 231–244.

681 Werkhausen A, Gløersen Ø, Nordez A, Paulsen G, Bojsen-Møller J & Seynnes OR (2023).
682 Linking muscle architecture and function in vivo: conceptual or methodological
683 limitations? *PeerJ* **11,** e15194.

684 Williams PE, Catanese T, Lucey EG & Goldspink G (1988). The importance of stretch and
685 contractile activity in the prevention of connective tissue accumulation in muscle. *J Anat*
686 **158,** 109–114.

687 Williams PE & Goldspink G (1978). Changes in sarcomere length and physiological properties
688 in immobilized muscle. *J Anat* **127,** 459–468.

689 Wisdom KM, Delp SL & Kuhl E (2015). Use it or lose it: multiscale skeletal muscle adaptation
690 to mechanical stimuli. *Biomech Model Mechanobiol* **14,** 195–215.

691 Woittiez RD, Heerkens YF, Huijing PA, Rijnsburger WH & Rozendal RH (1986). Functional
692 morphology of the M. Gastrocnemius medialis of the rat during growth. *J Morphol* **187,**
693 247–258.

694

695